

Aqueous Organometallic Chemistry: Synthesis, Structure, and Reactivity of the Water-Soluble Metal Hydride CpRu(PTA)₂H

Brian J. Frost* and Charles A. Mebi

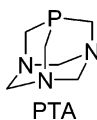
Department of Chemistry, University of Nevada, Reno, Nevada 89557

Received July 5, 2004

The reaction of CpRu(PTA)₂Cl (**1**) with KOH in methanol afforded the water-soluble hydride CpRu(PTA)₂H (**2**) in good yield. The solid-state structures of both CpRu(PTA)₂H and the previously reported CpRu(PTA)₂Cl are described and exhibit classic piano stool geometries. Complex **2** is one of a very few structurally characterized CpRu(PR₃)₂H compounds known and the only one that is water-soluble. The ruthenium hydride is stable and soluble (*S*_{25 °C} = 20 mg/mL) in deoxygenated water; however, the complex does react with chlorinated solvents to yield **1**. Complex **2** undergoes H/D exchange with D₂O, and the kinetics of this process were monitored by ³¹P NMR spectroscopy as a function of temperature. Activation parameters for the reaction of **2** with D₂O were obtained: $\Delta H^\ddagger = 68 \pm 2$ kJ/mol; $\Delta S^\ddagger = -94 \pm 7$ J/mol·K. A normal kinetic isotope effect of 7.9 was calculated for the H/D exchange reaction described here. These kinetic parameters suggest an associative mechanism with little Ru–H (or Ru–D) bond cleavage at the transition state. The reaction is postulated to occur via protonation of the hydride ligand of **2** by water followed by deprotonation by the resultant hydroxide. Finally DFT calculations were performed on all complexes and are consistent with the observed solid-state structures of **1** and **2**.

Introduction

Metal hydrides are an important class of molecules involved in numerous stoichiometric and catalytic processes.^{1,2} Cyclopentadienyl Ru(II) hydride complexes have received a great deal of attention in recent years due to their ability to catalyze various reactions. A number of half-sandwich ruthenium phosphine hydride complexes have been reported in the literature. Very few of these have been crystallographically characterized; of the structurally characterized CpRu(PR₃)₂H complexes none are water-soluble.^{3–8}



Our group is interested in metal complexes involving the neutral, water-soluble, and air-stable phosphine 1,3,5-triaza-7-phosphaadamantane (PTA), first synthe-

sized by Daigle.⁹ PTA has been used to make a variety of water-soluble metal complexes, which have shown moderate to good activity for a range of catalytic reactions.^{10–25} Bullock reported the first PTA-substituted half-sandwich metallocene metal hydride complex CpW(CO)₂PTA(H); however, this complex was found to be insoluble in water.²⁶ Dyson has reported the synthe-

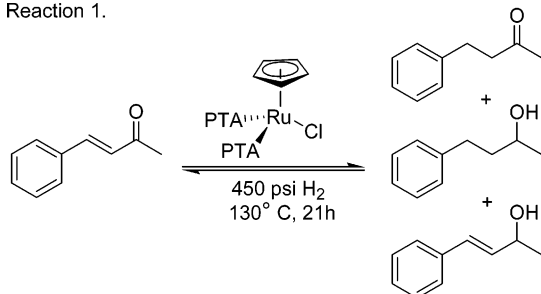
* Corresponding author. Tel: +1-775-784-1993. Fax: +1-775-784-6804. E-mail: Frost@chem.unr.edu.

- (1) Dedieu, A., Ed. *Transition Metal Hydrides*; VCH: New York, 1992.
- (2) Peruzzini, M.; Poli, R.; Eds. *Recent Advances in Hydride Chemistry*; Elsevier: New York, 2001.
- (3) Lemke, F. R.; Brammer, L. *Organometallics* **1995**, *14*, 3980–7.
- (4) Brammer, L.; Klooster, W. T.; Lemke, F. R. *Organometallics* **1996**, *15*, 1721–1727.
- (5) Smith, K. T.; Rømming, C.; Tilset, M. *J. Am. Chem. Soc.* **1993**, *115*, 8681–8689.
- (6) Bruce, M. I.; Butler, I. R.; Cullen, W. R.; Koutsantonis, G. A.; Snow, M. R.; Tiekink, E. R. T. *Aust. J. Chem.* **1988**, *41*, 963–969.
- (7) Litster, S. A.; Redhous, A. D.; Simpsons, S. J. *Acta Crystallogr.* **1992**, *C48*, 1661–1663.
- (8) Guan, H.; Iimura, M.; Magee, M. P.; Norton, J. R.; Janak, K. E. *Organometallics* **2003**, *22*, 4084–4089.

- (9) Daigle, D. J.; Pepperman, A. B. Jr.; Vail, S. L. *J. Heterocycl. Chem.* **1974**, *11*, 407–408.
- (10) Joó, F.; Laurency, G.; Karady, P.; Elek, J.; Nadasdi, L.; Roulet, R. *Appl. Organomet. Chem.* **2000**, *14*, 857–859.
- (11) Laurency, G.; Joó, F.; Nadasdi, L. *Inorg. Chem.* **2000**, *39*, 5083–5088.
- (12) Pruchnik, F. P.; Smolenski, P. *Appl. Organomet. Chem.* **1999**, *13*, 829–836.
- (13) Nadasdi, L.; Joó, F. *Inorg. Chim. Acta* **1999**, *293*, 218–222.
- (14) Pruchnik, F. P.; Smolenski, P.; Galdecka, E.; Galdecki, Z. *New J. Chem.* **1998**, *22*, 1395–1398.
- (15) Darensbourg, D. J.; Decuir, T. J.; Reibenspies, J. H. *Aqueous Organometallic Chemistry and Catalysis*; Horvath, I. T., Joó, F., Eds.; High Technology; Kluwer: Dordrecht, The Netherlands, 1995; pp 61–80.
- (16) Darensbourg, D. J.; Stafford, N. W.; Joó, F.; Reibenspies, J. H. *J. Organomet. Chem.* **1995**, *488*, 99–108.
- (17) Pruchnik, F. P.; Smolenski, P.; Raksa, I. *Polym. J. Chem.* **1995**, *69*, 5–8.
- (18) Kovacs, J.; Todd, T. D.; Reibenspies, J. H.; Joó, F.; Darensbourg, D. J. *Organometallics* **2000**, *19*, 3963–3969.
- (19) Pruchnik, F. P.; Smolenski, P.; Wajda-Hermanowicz, K. *J. Organomet. Chem.* **1998**, *570*, 63–69.
- (20) Cermak, J.; Kvicálova, M.; Blechta, V. *Collect. Czech. Chem. Commun.* **1997**, *62*, 355–363.
- (21) Darensbourg, D. J.; Joó, F.; Kannisto, M.; Katho, A.; Reibenspies, J. H.; Daigle, D. J. *Inorg. Chem.* **1994**, *33*, 200–208.
- (22) Darensbourg, D. J.; Joó, F.; Kannisto, M.; Katho, A.; Reibenspies, J. H. *Organometallics* **1992**, *11*, 1990–1993.
- (23) Joó, F.; Nadasdi, L.; Benyei, A. Cs.; Darensbourg, D. J. *J. Organomet. Chem.* **1996**, *512*, 45–50.
- (24) Joó, F.; Laurency, G.; Nadasdi, L.; Elek, J. *Chem. Commun.* **1999**, 971–972.
- (25) Benyei, A. Cs.; Lehel, S.; Joó, F. *J. Mol. Catal. A: Chem.* **1997**, *116*, 349–354.

sis, characterization, and reactivity of a series of $[(\eta^6\text{-arene})\text{Ru}(\text{PTA})_2\text{X}]^+$ and $(\eta^6\text{-arene})\text{Ru}(\text{PTA})\text{X}_2$ complexes, where X = Cl, Br, I, NCS and arene = C₆H₆, cymene.^{27–29} Kathó et al. have more recently reported the catalytic activity of $[(\eta^6\text{-C}_6\text{H}_6)\text{Ru}(\text{PTA})_2\text{H}]^+$ and $[(\eta^6\text{-cymene})\text{Ru}(\text{PTA})_2\text{H}]^+$ for the hydrogenation of bicarbonate in water, although neither of these hydrides was isolated.³⁰ Peruzzini et al. reported the synthesis of CpRu(PTA)₂Cl and Cp*Ru(PTA)₂Cl; at high temperatures and pressures of hydrogen gas these compounds were found to be active in the biphasic hydrogenation of benzylidene acetone, reaction 1.³¹ In the course of this study, Peruzzini et al. report spectroscopic data on a new ruthenium hydride, CpRu(PTA)₂H.

Reaction 1.



Herein, we report details of the synthesis, isolation, reactivity, and crystal structure of CpRu(PTA)₂H, to the best of our knowledge the first structurally characterized water-soluble CpRu(PR₃)₂H compound. Also reported are the details of a H/D exchange reaction CpRu(PTA)₂H undergoes with D₂O.

Experimental Section

Materials and Methods. Unless otherwise noted all manipulations were performed on a double-manifold Schlenk vacuum line under an atmosphere of nitrogen or in a nitrogen-filled glovebox. Tetrakis(hydroxymethyl) phosphonium chloride was obtained from Cytec and used as received. RuCl₃·xH₂O, D₂O, KOH, PPh₃, dicyclopentadiene, and 1,5-cyclooctadiene (COD) were purchased from commercial sources and used as received. 1,3,5 triaza-7-phosphaadamantane (PTA),^{9,32} CpRu(COD)Cl,³³ CpRu(PPh₃)₂Cl,³⁴ and CpRu(PTA)₂Cl³¹ were prepared according to the literature procedures. Solvents were freshly distilled from standard drying reagents or dried with activated molecular sieves. Water was distilled and deoxygenated prior to use. NMR spectra were recorded on either a Varian Unity Plus 500 FT-NMR spectrometer, a GN 300 FT-NMR/Scorpio spectrometer, or a QE 300 FT-NMR/Aquarius spectrometer. Proton spectra were referenced to residual solvent relative to TMS with the exception of aqueous spectra,

(26) Shafiq, F.; Szalda, D. J.; Creutz, C.; Bullock, R. M. *Organometallics* **2000**, *19*, 824–833.

(27) Allardyce, C. S.; Dyson, P. J.; Ellis, D. J.; Heath, S. L. *Chem. Commun.* **2001**, 1396–1397.

(28) Dyson, P. J.; Ellis, D. J.; Henderson, W.; Laurency, G. *Adv. Synth. Catal.* **2003**, *345*, 216–221.

(29) Allardyce, C. S.; Dyson, P. J.; Ellis, D. J.; Salter, P. A.; Scopelliti, R. *J. Organomet. Chem.* **2003**, *668*, 35–42.

(30) Horvath, H.; Laurency, G.; Katho, A. *J. Organomet. Chem.* **2004**, *689*, 1036–1045.

(31) Akbayeva, D. N.; Gonsalvi, L.; Oberhauser, W.; Peruzzini, M.; Vizza, F.; Brueggeller, P.; Romerosa, A.; Sava, G.; Bergamo, A. *Chem. Commun.* **2003**, 264–265.

(32) Daigle, D. J. *Inorg. Synth.* **1998**, *32*, 40–45.

(33) Albers, M. O.; Liles, D. C.; Robinson, D. J.; Shaver, A.; Singleton, E.; Wiege, M. B.; Boeyens, J. C. A.; Levendis, D. C. *Organometallics* **1986**, *5*, 2321–2327.

(34) Joslin, F. L.; Mague, J. T.; Roundhill, D. M. *Organometallics* **1991**, *10*, 521–524.

Table 1. Summary of Data Collection, Solution, and Refinement Parameters for 1 and 2

	1	2
empirical formula	(C ₅ H ₅)Ru(PC ₆ H ₁₂ -N ₃) ₂ Cl·2H ₂ O	(C ₅ H ₅)Ru(PC ₆ H ₁₂ -N ₃) ₂ H
fw	547.92	481.48
T (K)	123(2) K	100(2) K
wavelength (Å)	0.71073	0.71073
cryst syst/space group	monoclinic, Cc	monoclinic, P2(1)/n
a (Å)	13.037(2)	16.3954(16)
b (Å)	23.864(4)	6.4753(6)
c (Å)	7.3899(11)	19.8608(19)
α (deg)	90°	90°
β (deg)	105.856(2)°	113.122(2)°
γ (deg)	90°	90°
volume (Å ³)	2211.7(6)	1939.1(3)
Z	4	4
D _{calc} (Mg/m ³)	1.646	1.649
absorp coeff (mm ⁻¹)	1.001	0.988
cryst size (mm ³)	0.275 × 0.060 × 0.011	0.65 × 0.17 × 0.09
θ range for data collection (deg)	1.71 to 27.74	2.06 to 32.30
index ranges	-16 ≤ h ≤ 15, -31 ≤ k ≤ 17, -9 ≤ l ≤ 9	-24 ≤ h ≤ 24, -9 ≤ k ≤ 9, -29 ≤ l ≤ 29
no. of reflns collected/unique	6399/3907	32 461/6869
absorp corr	[R(int) = 0.0680]	[R(int) = 0.0371]
no. of data/restraints/params	SADABS	SADABS
goodness-of-fit on F ²	3907/2/262	6869/0/355
final R indices	0.965	1.058
[I > 2σ(I)]	R ₁ = 0.0448, wR ₂ = 0.0848	R ₁ = 0.0460, wR ₂ = 0.1215
R indices (all data)	R ₁ = 0.0629, wR ₂ = 0.0899	R ₁ = 0.0522, wR ₂ = 0.1273

which were referenced to an external standard of sodium 2,2-dimethyl-2-silapentane-5-sulfonate (DSS). Phosphorus chemical shifts are relative to an external reference of 85% H₃PO₄ in D₂O with positive values downfield of the reference. IR spectra were recorded on a Perkin-Elmer 2000 FT-IR spectrometer, in a 0.1 mm CaF₂ cell for solutions or as a KBr pellet for solid samples.

Crystal Structure of CpRu(PTA)₂Cl (1). CpRu(PTA)₂Cl (1) was synthesized as reported in the literature.³¹ X-ray quality crystals were obtained by layering a CH₂Cl₂ solution of CpRu(PTA)₂Cl with methanol and diethyl ether. Yellow needles were obtained after 1 day. A crystal suitable for X-ray diffraction was selected and mounted under oil on a glass fiber. Crystallographic data and data collection parameters are listed in Table 1.

Alternative Synthesis of 1. A CH₂Cl₂ (2 mL) solution of CpRu(COD)Cl (20 mg, 0.065 mmol) and PTA (20 mg, 0.13 mmol) was stirred under N₂ for 1 h. The solvent was then removed under vacuum, resulting in an orange powder, which upon washing with hexanes (2 × 5 mL) afforded 1 in 98% yield (33 mg). Spectroscopic data for 1 obtained via this method is identical to that reported for the literature preparation of 1.³¹

Synthesis of CpRu(PTA)₂H (2). CpRu(PTA)₂Cl (0.05 g, 0.097 mmol) and KOH (0.08 g, 1.43 mmol) were refluxed for 45 min in 15 mL of methanol under nitrogen or until disappearance of the yellow color was observed. The solvent was then removed under vacuum and the resulting solid extracted with 2 × 10 mL of freshly distilled THF. Removal of the THF under vacuum afforded 0.025 g (53%) of 2 as a white powder. ¹H NMR (300 MHz, CD₂Cl₂): δ 4.69 (s, 5H, Cp); 4.49, 4.40 (AB spin system, ²J(H_AH_B) = 12.5 Hz, 12H NCH₂N); 3.75 (s, 12H, PCH₂N); -14.36 ppm (t, ²J_{PH} = 36.6 Hz, 1H, RuH). ¹H NMR (300 MHz, D₂O): δ 4.79 (s, 5H, Cp); 4.54 (s, 12H NCH₂N); 3.81 (s, 12H, PCH₂N); -14.61 ppm (t, ²J_{PH} = 36.6 Hz, 1H, RuH). ³¹P NMR: δ -12.0 ppm (d, ²J_{PH} = 36.6 Hz). IR (KBr): ν(Ru–H) 1927 (br) and 1903 (br) cm⁻¹; IR (THF): ν(Ru–H) 1891 (br) cm⁻¹.

Crystals of $\text{CpRu(PTA)}_2\text{H}$ suitable for X-ray diffraction were obtained from a concentrated THF solution of **2** layered with hexanes and maintained at room temperature in a drybox for 2 days. Due to the extreme air sensitivity of this compound, the crystals were placed under paratone oil in the drybox, then carried quickly to the microscope for mounting on a glass fiber. Crystallographic data and data collection parameters are listed in Table 1.

Synthesis of $\text{CpRu(PTA)}_2\text{D}$ (2D**).** $\text{CpRu(PTA)}_2\text{H}$ (0.05 g) was dissolved in D_2O and stirred for 24 h under nitrogen. The resultant solution was pulled dry under vacuum to afford $\text{CpRu(PTA)}_2\text{D}$ in 98% yield and >98%D by ^1H and ^{31}P NMR. ^1H NMR (300 MHz, D_2O): δ 4.79 (s, 5H, Cp); 4.54 (s, 12H NCH_2N); 3.81 (s, 12H, PCH_2N). $^{31}\text{P}\{^1\text{H}\}$ NMR: δ -11.9 ppm (t , $^2J_{\text{PD}} = 4.65$ Hz). IR (KBr): $\nu(\text{Ru}-\text{D})$ 1383 (br) cm^{-1} .

Kinetics Measurements. The rate of H/D exchange of **2** was determined by dissolving 0.005 g (0.010 mmol) of **2** in 1.0 mL of D_2O in an NMR tube. This NMR tube was then quickly placed into a temperature-equilibrated NMR spectrometer. The rates of H/D exchange were monitored by following the disappearance of Ru-H and the appearance of the Ru-D by ^{31}P NMR. This procedure was repeated for a variety of temperatures (25, 35, 45, 55, 60 °C) to obtain activation parameters. The isotope effect was determined in an analogous experiment except $\text{CpRu(PTA)}_2\text{D}$ was dissolved in H_2O and the reaction followed by ^{31}P NMR spectroscopy.

Computational Details. All calculations were run on a Beowulf cluster of 16 dual processor computers operating under Linux. Theoretical calculations were performed using the Gaussian 03 program package employing the LANL2DZ basis set of Wadt and Hay^{35,36} as implemented in Gaussian 03.³⁷ Density functional (DFT) calculations were carried out on all complexes using Becke's three-parameter hybrid method³⁸ coupled to the correlation functional of Lee, Yang, and Parr (B3LYP).³⁹ Frequency calculations were performed on all optimized structures in order to establish the nature of the extrema and to calculate values for ΔH and ΔG .

Results and Discussion

Structure of $\text{CpRu(PTA)}_2\text{Cl}$. $\text{CpRu(PTA)}_2\text{Cl}$ (**1**) was prepared, as reported in the literature, through exchange of PPh_3 for PTA in $\text{CpRu(PPh}_3)_2\text{Cl}$.³¹ Alternatively, **1** can also be synthesized by substitution of cyclooctadiene by PTA in CpRu(COD)Cl . The solid-state structure of complex **1** was determined by X-ray crystallography. Yellow needles of $\text{CpRu(PTA)}_2\text{Cl}$ suitable for X-ray diffraction were obtained by layering a CH_2Cl_2 solution of $\text{CpRu(PTA)}_2\text{Cl}$ with methanol and diethyl ether. A thermal ellipsoid view of **1** is depicted in Figure 1, along with the atomic numbering scheme and selected

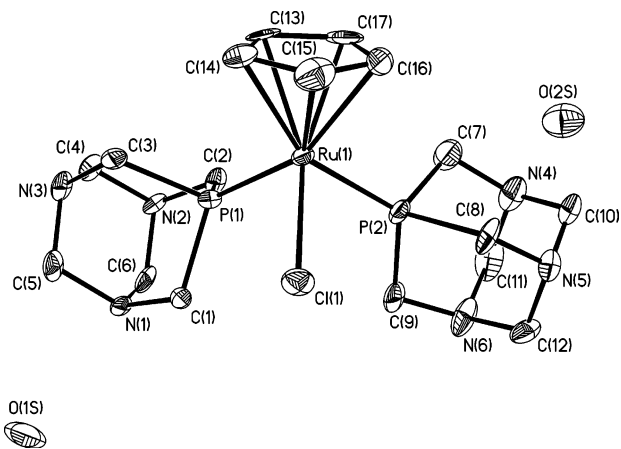


Figure 1. Thermal ellipsoid representation of $\text{CpRu(PTA)}_2\text{Cl}\cdot 2\text{H}_2\text{O}$ (**1**) including the atomic numbering scheme. Hydrogen atoms have been omitted for clarity. Thermal ellipsoids are drawn at 50% probability. Selected bond lengths (Å) and angles (deg): Ru(1)–P(1) = 2.258(3), Ru(1)–P(2) = 2.247(3), Ru(1)–Cl(1) = 2.4452(15), Ru(1)–Cp_{centroid} = 1.846(7); P(1)–Ru(1)–P(2) = 96.85(5), P(1)–Ru(1)–Cl(1) = 91.61(7), P(2)–Ru(1)–Cl(1) = 86.46(7).

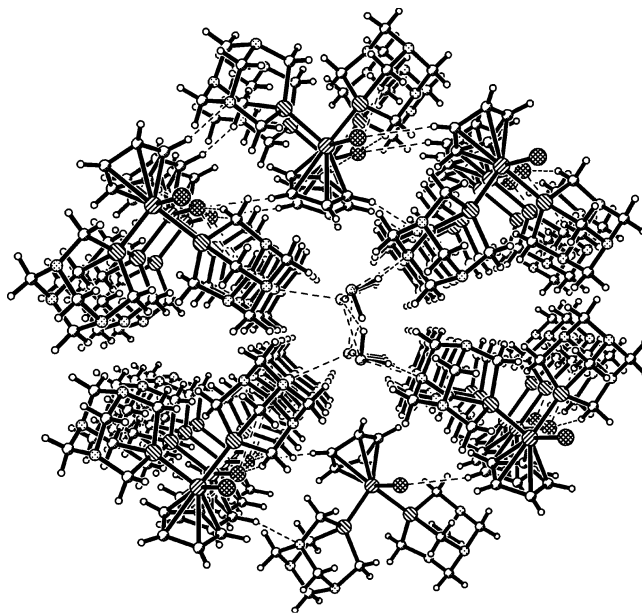


Figure 2. Packing diagram of **1**, looking down the c axis, showing the solvent channel created by the packing of $\text{CpRu(PTA)}_2\text{Cl}$.

bond distances and bond angles. The piano stool complex **1** consists of a cyclopentadiene ligand (Cp) bound to a ruthenium with two PTA ligands and the chloride. The PTA ligands of **1** are bound, as expected, through phosphorus and are tilted away from the chloride ligand. The angle between the plane defined by the Cp ligand and the plane defined by Ru(1), P(1), and P(2) in compound **1** was found to be 55.3°. Ru(1) was measured to be 1.844 Å from the plane defined by the Cp ligand, consistent with a normal Ru–Cp distance. The (N)C–N distances of the PTA ligands are found to be 1.49 Å, consistent with nonprotonated PTA ligands.¹⁵

Two equivalents of water cocrystallize with **1** and are found in a channel formed by the packing of **1**. Figure 2 contains a representation of the packing diagram showing the water molecules hydrogen bound to the nitrogen of the PTA ligands pointing toward the center

(35) Wadt, W. R.; Hay, P. J. *J. Chem. Phys.* **1985**, *82*, 284–298.

(36) Hay, P. J.; Wadt, W. R. *J. Chem. Phys.* **1985**, *82*, 270–283.

(37) Frisch, M. J.; Trucks, G. W.; Schlegel, H. B.; Scuseria, G. E.; Robb, M. A.; Cheeseman, J. R.; Montgomery, J. A., Jr.; Vreven, T.; Kudin, K. N.; Burant, J. C.; Millam, J. M.; Iyengar, S. S.; Tomasi, J.; Barone, V.; Mennucci, B.; Cossi, M.; Scalmani, G.; Rega, N.; Petersson, G. A.; Nakatsuji, H.; Hada, M.; Ehara, M.; Toyota, K.; Fukuda, R.; Hasegawa, J.; Ishida, M.; Nakajima, T.; Honda, Y.; Kitao, O.; Nakai, H.; Klene, M.; Li, X.; Knox, J. E.; Hratchian, H. P.; Cross, J. B.; Adamo, C.; Jaramillo, J.; Gomperts, R.; Stratmann, R. E.; Yazyev, O.; Austin, A. J.; Cammi, R.; Pomelli, C.; Ochterski, J. W.; Ayala, P. Y.; Morokuma, K.; Voth, G. A.; Salvador, P.; Dannenberg, J. J.; Zakrzewski, V. G.; Dapprich, S.; Daniels, A. D.; Strain, M. C.; Farkas, O.; Malick, D. K.; Rabuck, A. D.; Raghavachari, K.; Foresman, J. B.; Ortiz, J. V.; Cui, Q.; Baboul, A. G.; Clifford, S.; Cioslowski, J.; Stefanov, B. B.; Liu, G.; Liashenko, A.; Piskorz, P.; Komaromi, I.; Martin, R. L.; Fox, D. J.; Keith, T.; Al-Laham, M. A.; Peng, C. Y.; Nanayakkara, A.; Challacombe, M.; Gill, P. M. W.; Johnson, B.; Chen, W.; Wong, M. W.; Gonzalez, C.; Pople, J. A. *Gaussian 03*, Revision B.02; Gaussian, Inc.: Pittsburgh, PA, 2003.

(38) Becke, A. D. *Phys. Rev. A* **1988**, *38*, 3098–3100.

(39) Lee, C.; Yang, W.; Parr, R. G. *Phys. Rev. B* **1988**, *37*, 785.

Table 2. Comparison of Selected Bond Lengths [Å] and Angles [deg] for **1** with Those Reported for Cp*Ru(PTA)₂Cl and Those Calculated Using DFT

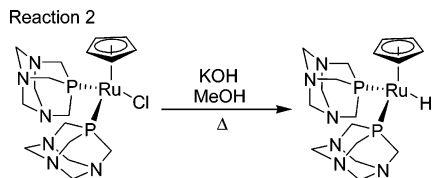
	CpRu(PTA) ₂ Cl		Cp*Ru(PTA) ₂ Cl
	DFT	X-ray	X-ray ^a
Ru–Cl	2.53	2.445(2)	2.465(2); 2.468(2)
Ru–P(1)	2.389	2.258(3)	2.284(1); 2.285(2)
Ru–P(2)	2.388	2.247(3)	2.285(2); 2.287(2)
Ru–C _{cp-av}	2.295	2.197(7)	2.211(6); 2.208(8)
P(1)–Ru–P(2)	96.2	96.85(5)	93.30(5); 93.37(7)
P(1)–Ru–Cl	86.68	91.61(7)	90.69(6); 90.94(9)
P(2)–Ru–Cl	82.95	86.46(7)	84.38(6); 84.27(8)

^a See ref 31; note two molecules in the asymmetric unit.

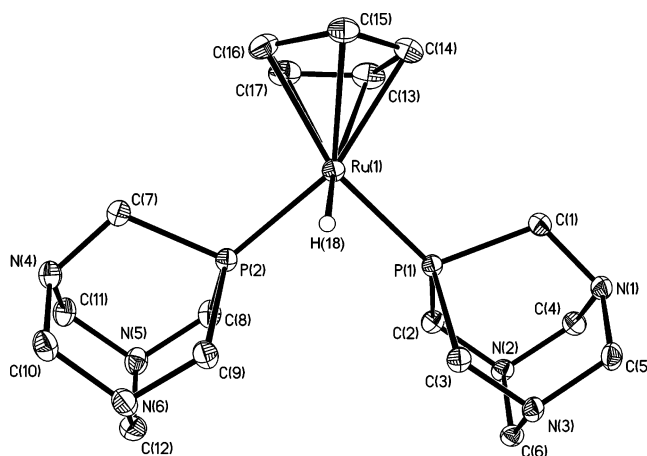
of the channel. Two N···O separations are observed, both within standard hydrogen bonding distances: O(2)···N(4) = 2.779 Å and O(1)···N(1) = 2.908 Å.

A comparison of the bond lengths for CpRu(PTA)₂Cl and Cp*Ru(PTA)₂Cl is presented in Table 2, along with DFT calculated bond lengths and angles, Cp* = Me₅C₅[−]. DFT calculations yielded bond lengths that are ~0.1 Å longer than the experimentally determined bond lengths. The structures of **1** and Cp*Ru(PTA)₂Cl are virtually identical. The major difference between the two structures is a slight increase in the P–Ru–P angle in **1** with respect to the Cp* analogue and a minor decrease in the Ru–P and Ru–Cl bond distances in **1**. These observations are consistent with the greater electron-donating and steric requirements of Cp* versus Cp.

Preparation of CpRu(PTA)₂H. The water-soluble CpRu(PTA)₂H (**2**) (*S*₂₅ °C = 20 mg/mL) was obtained in good yield by reaction of **1** with KOH in methanol under reflux, reaction 2. This reaction presumably occurs through a Ru–OMe complex, which undergoes β-hydride elimination yielding the Ru–H and formaldehyde. Extraction of the resulting solid with THF afforded the off-white **2** in 53% yield. The ³¹P NMR spectrum of **2** contains a doublet centered at −12.0 ppm in D₂O (²J_{H–P} = 36.6 Hz). The ¹H NMR spectrum of **2** varies with solvent. In CD₂Cl₂ the resonance for the Cp protons appears as a sharp singlet at 4.69 ppm. The NCH₂N protons of PTA exhibit a classic AB pattern centered at 4.49 and 4.40 ppm with a ²J_{(HaHb)}} = 12.5 Hz. The PCH₂N protons of PTA appear as a slightly broad singlet at 3.75 ppm. The hydride resonance is observed as a triplet at −14.36 ppm ²J_{(HP)}} = 36.6 Hz. In D₂O the Cp and PCH₂N resonances shift slightly to 4.54 and 3.81 ppm, respectively. The hydride signal in D₂O shifts upfield to −14.61 ppm. The NCH₂N resonances in D₂O no longer appear as an AB pattern but are observed as a singlet at 4.54 ppm.



The solid-state structure of **2** was determined by X-ray crystallography. Pale tan (almost colorless) crystals of CpRu(PTA)₂H suitable for X-ray diffraction were obtained from a concentrated THF solution of **2** layered with hexanes and maintained at room temperature in a drybox for 2 days. A thermal ellipsoid view of **2** is depicted in Figure 3, along with the atomic numbering

**Figure 3.** Thermal ellipsoid representation of CpRu(PTA)₂H (**2**) including the atomic numbering scheme. Hydrogen atoms have been omitted for clarity. Thermal ellipsoids are drawn at 50% probability. Selected bond lengths (Å) and angles (deg): Ru(1)–P(1) = 2.2220(7), Ru(1)–P(2) = 2.2267(7), Ru(1)–H(18) = 1.68(7), Ru(1)–Cp_{centroid} = 1.896(3); P(1)–Ru(1)–P(2) = 95.68(2), P(1)–Ru(1)–H(18) = 81(2), P(2)–Ru(1)–H(18) = 73(2).**Table 3.** Comparison of Selected Bond Lengths [Å] and Angles [deg] of the DFT Calculated Structure of **2** and the Experimentally Determined Structure

	DFT	X-ray
Ru–H	1.62	1.68(7)
Ru–P	2.35	2.2220(7); 2.2267(7)
Ru–C _{cp-av}	2.34	2.250(3)
P(1)–Ru–P(2)	97.33	95.68(2)
P(1)–Ru–H(18)	83.4	81(2)
P(2)–Ru–H(18)	83.1	73(2)

scheme. All hydrogens were located in the difference map. Selected bond distances and bond angles are found in Table 3 along with data from the DFT calculated structure. DFT calculations yielded bond lengths ~0.1 Å longer than the experimentally determined bond lengths. Important to note is that the calculated Ru–H position is virtually identical to the experimentally determined Ru–H position. These calculations help to serve as evidence that we have indeed found the hydride in the difference map of **2**. The piano stool complex **2** consists of a cyclopentadiene ligand (Cp) bound to a ruthenium with two PTA ligands and the hydride. The PTA ligands of **2** are bound, as expected, through phosphorus and are tilted away from the hydride ligand, as described by Lemke and Brammer, indicating a third ligand (the hydride).³ The Ru–P bond lengths of 2.22 Å for **2** are consistent with other published Ru–P distances in similar complexes. The range of Ru–P distances for the small number of structurally characterized CpRu(PR₃)₂H complexes is 2.21–2.25 Å.^{3–8} The Ru(1)–H(18) bond distance of 1.68(7) Å agrees well with the previously reported distances in similar complexes, where Ru–H distances have been reported to be between 1.56 and 1.73 Å.^{5–8} Most importantly the Ru–H bond length reported here for **2** agrees well with the neutron diffraction data for CpRu(PMe₃)₂H, where the Ru–H bond distance was found to be 1.630(4) Å.⁴ The distance from Ru(1) to the Cp centroid is a normal 1.896(3) Å. The (N)C–N distances of the PTA ligands are 1.469(3) Å, consistent with nonprotonated PTA ligands.¹⁵ The angle between the plane defined by the

Cp ligand and the plane defined by Ru(1), P(1), and P(2), the Cp–ML₂ angle, was found to be 67.8°, ~12° greater than the value for complex **1**, consistent with the mean value (67.6°) reported for a series of Cp'M(L)₂H complexes.³ The change in Cp–ML₂ angle from **1** to **2** can be ascribed to both the smaller steric requirement of H[−] versus Cl[−] and an electronic effect. On the basis of electronic effects the PTA ligands would be expected to move toward the hydride, as H[−] is a better σ donor than Cl[−].⁴⁰

A comparison of the crystallographic parameters of **2** with CpRu(PMe₃)₂H shows the two compounds to be very similar. The P–Ru–P angle is virtually identical, 96.0° for CpRu(PMe₃)₂H and 95.68° for **2**. The Cp–ML₂ angle for CpRu(PMe₃)₂H at 67.1° is also very similar to that observed for **2**, 67.8°. The slight difference can be related to the difference in the Tolman cone angle for the two phosphines (PTA = 103°,^{41,42} PMe₃ = 118°⁴³). For comparison the P–Ru–P and Cp–ML₂ angles for CpRu(PPh₃)₂H were found to be 100.7° and 65.5°, respectively, significantly different than found in **2**, again due to the differences in cone angle between the two phosphines. The P–Ru–P angle is opened up considerably when compared to most of the CpRu(P–P)H complexes recently reported by Norton, where P–Ru–P angles ranged from 72.0° for CpRu(DPPM)H, to 84.5° for CpRu(DPPE)H, to 94.0° for CpRu(DPPB)H, where DPPM = diphenylphosphinomethane, DPPE = diphenylphosphinoethane, and DPPB = diphenylphosphinobutane.⁸ The Cp–ML₂ angles for these CpRu(P–P)H complexes were found to be 72.1° for CpRu(DPPM)H, 69.7° for CpRu(DPPE)H, and 65.6° for CpRu(DPPB)H, decreasing with increasing bite angle. Norton has recently correlated the P–Ru–P bite angles of the CpRu(P–P)H complexes above with the rates of hydride transfer to iminium cations.⁸ The P–Ru–P and Cp–ML₂ angles suggest that **2** should have approximately the same hydride transfer ability as CpRu(DPPB)H, which was not capable of transferring H[−] to an iminium cation.⁸

The IR spectrum of **2** was obtained as a KBr pellet. We have assigned two peaks to the Ru–H stretching mode: 1927 and 1903 cm^{−1}. The two peaks in the solid-state IR arise from well-known solid effects.^{44,45} In the crystal lattice of **2** there are two different orientations of the Ru–H dipole, leading to two different IR frequencies (Figure 4). In solution (THF) the expected single ν (Ru–H) frequency is observed at 1891 cm^{−1}. In the IR spectrum of CpRu(PTA)₂D (**2D**) the peaks at 1927 and 1903 cm^{−1} are no longer visible, and a new peak at 1383 cm^{−1} corresponding to ν (Ru–D) is observed. The isotopic shift is consistent with the value expected from Hooke's law for a pure Ru–H stretching mode (calculated shift 554 cm^{−1}). The DFT calculated IR spectrum of **2** exhibits a ν (Ru–H) of 1957 cm^{−1}, in good agreement with the experimentally observed Ru–H stretching frequency.

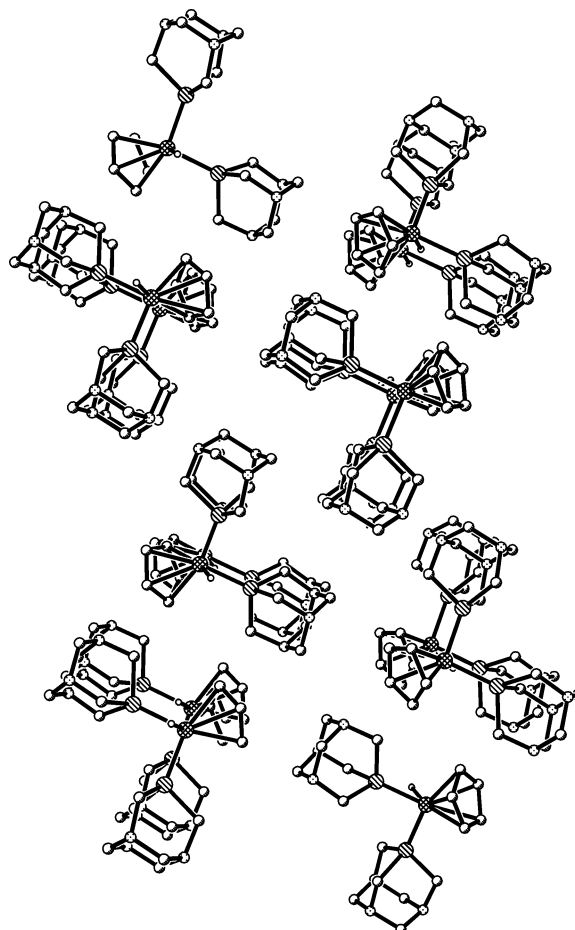
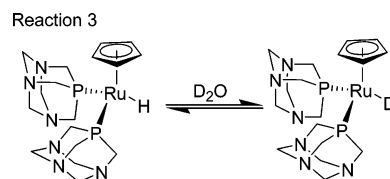


Figure 4. Packing diagram of **2**, looking down the *b* axis.

Reactivity of CpRu(PTA)₂H. CpRu(PTA)₂H is stable in deoxygenated water. The pH of a 1.3 × 10^{−3} M solution of **2** is ~8.5 due to the amine functionalities on the PTA ligands. Aqueous solutions of **2** may be kept for weeks without observable decomposition. Upon exposure to air, **2** quickly decomposed within ~30 min, during which time a color change from colorless to yellow to black. As with many metal hydrides, **2** reacts with chlorinated solvents such as CH₂Cl₂ and CHCl₃, rapidly yielding **1**, precluding the use of chlorinated solvents with **2**, at least without a radical trap/inhibitor such as TEMPO (2,2,6,6-tetramethyl-1-piperidinyloxy) present.⁸



Compound **2** undergoes H/D exchange with the solvent (D₂O), *t*_{1/2} = 127 min at 25 °C, reaction 3. The reaction of **2** with D₂O was followed by ³¹P{¹H} NMR spectroscopy. Over time the phosphorus resonance (*s*, −12.0 ppm) disappears, and it is replaced by a second phosphorus resonance at almost the same chemical shift (*t*, −11.9 ppm, ²*J*_{PD} = 4.65 Hz), Figure 5. H/D exchange was not observable in CD₃OD over the course of two weeks.

We have examined the pseudo-first-order kinetics of this process over a range of temperatures (25–60 °C),

(40) Elian, M.; Hoffmann, R. *Inorg. Chem.* **1975**, *14*, 1058–1076.

(41) Darensbourg, D. J.; Robertson, J. B.; Larkins, D. L.; Reibenspies, J. H. *Inorg. Chem.* **1999**, *38*, 2473–2481.

(42) DeLerno, J. R.; Trefonas, L. M.; Darensbourg, M. Y.; Majeste, R. J. *Inorg. Chem.* **1976**, *15*, 816–819.

(43) Tolman, C. A. *Chem. Rev.* **1977**, *77*, 313–348.

(44) Drago, R. S. *Physical Methods for Chemists*, 2nd ed.; Saunders: Philadelphia, 1992.

(45) Krimm, S. *Infrared Spectroscopy and Molecular Structure*; Elsevier: New York, 1963; Chapter 8.

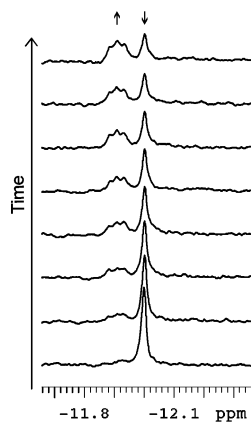


Figure 5. $^{31}\text{P}\{^1\text{H}\}$ NMR spectra over time for the reaction of **2** with D_2O at 35°C .

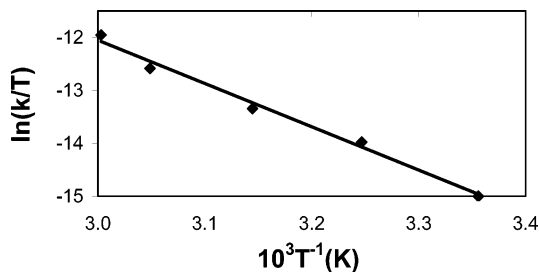


Figure 6. Eyring plot for the H/D exchange between **2** and D_2O .

Table 4. Observed Pseudo-First-Order Rate Constants for the H/D Exchange in Complex **2, as a Function of Temperature^a**

complex	temp, $^\circ\text{C}$	k_{obs} , s^{-1} ($\times 10^4$)
2	25	0.91 ^b
	35	2.6 ^b
	45	5.1
	55	11.2
	60	21.4
2D	35	12.4

^a In D_2O . ^b Average rate constant of two kinetics experiments at different $[\mathbf{2}]$.

Table 4. Activation parameters were obtained from an Eyring plot of the data, Figure 6: $\Delta H^\ddagger = 68 \pm 2$ kJ/mol; $\Delta S^\ddagger = -94 \pm 7$ J/mol·K. From an Arrhenius plot of the data an activation barrier (E_a) of 71 ± 3 kJ/mol is obtained. The kinetics of the reaction of $\text{CpRu}(\text{PTA})_2\text{D}$ (**2D**) with H_2O were also followed by ^{31}P NMR spectroscopy. **2D** was dissolved in H_2O , and the disappearance of the ^{31}P NMR signal at -11.9 ppm was monitored at 35°C . The observed rate constant for the disappearance of **2D** was found to be $\sim 5\times$ larger than that for the disappearance of **2**. The large and negative value of ΔS^\ddagger and the relatively small positive value for ΔH^\ddagger suggest an associative mechanism for the H/D exchange of **2** in D_2O with concomitant bond breaking/bond making in the transition state. Under the reaction conditions described (i.e., pseudo-first-order) the rate constant for the exchange process was not dependent on $[\mathbf{2}]$, excluding a mechanism involving two metal centers. On the basis of the data presented above the likely mechanism involves protonation of **2** by water (or D_2O), forming a Ru dihydride/dihydrogen intermediate. The intermediate is then deprotonated by the resultant hydroxide ion generated during the protonation step. Deprotonation may lead to either H/D exchange or reversion back to

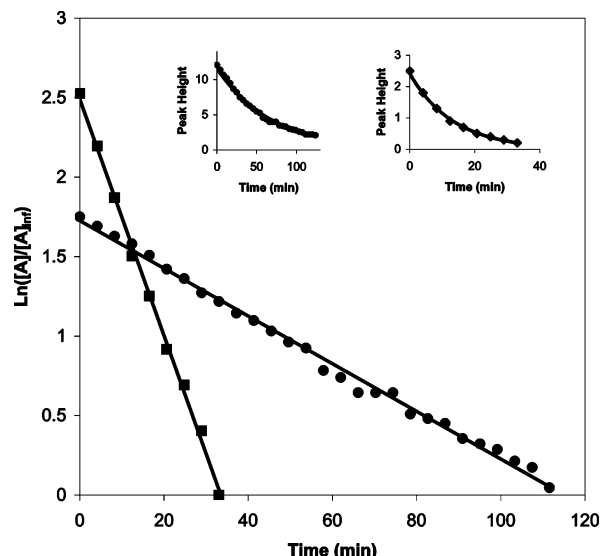
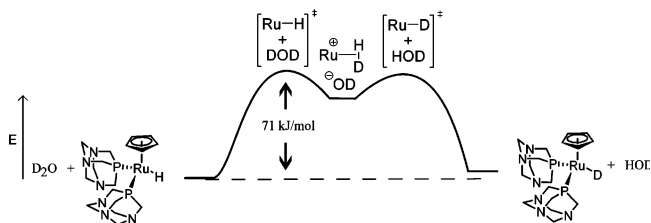


Figure 7. Plot of $\ln([A]/[A]_0)$ versus t for the H/D exchange reaction of **2** (●) and **2D** (■) based on ^{31}P NMR peak heights at 35°C . The pseudo-first-order rate constants (k_{obs}) are $2.6 \times 10^{-4} \text{ s}^{-1}$ for reaction of **2** with D_2O and $1.24 \times 10^{-3} \text{ s}^{-1}$ for the reaction of **2D** with H_2O . Insets show the exponential decay (peak height versus time) of **2** (●) and **2D** (■).

Scheme 1

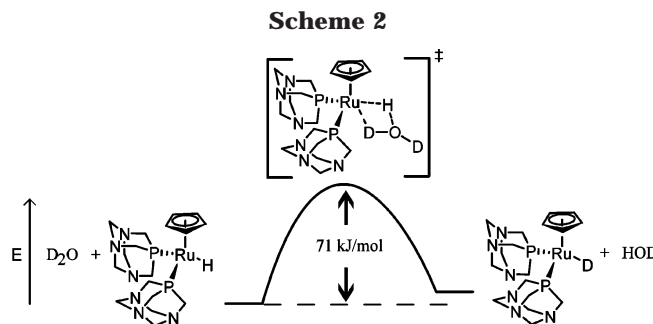


the starting material, Scheme 1. It has been reported that for many $\text{M}-\text{H}$ compounds the hydride is the kinetic site of protonation.⁴⁶ Thus, we speculate that the intermediate in Scheme 1 is likely to be $\text{Ru}(\eta^2\text{-H}_2)^+$ and not $\text{Ru}(\text{H})_2^+$. A second conceivable mechanism involves an anion-stabilized dihydride (or dihydrogen), where the transition state contains a counteranion (hydroxide) bridging both the entering and leaving proton, Scheme 2.^{47,48} Both of these mechanisms account for the associative character of the reaction and incorporate significant bond breaking and bond formation in the transition state. We have observed that protonation of **2** leads to an observable complex **2H**⁺, which appears to be $\text{CpRu}(\text{PTA})_2(\text{H})_2^+$, presumably formed by rear-

(46) See for example: (a) Kristjánssdóttir, S. S.; Norton, J. R. *Acidity of Hydrido Transition Metal Complexes in Solution*. In *Transition Metal Hydrides*; Dedieu, A., Ed.; VCH: New York, 1992. (b) Jessop, P. G.; Morris, R. H. *Coord. Chem. Rev.* **1992**, *121*, 155–284. (c) Heinekey, D. M.; Oldham, W. J., Jr. *Chem. Rev.* **1993**, *93*, 913. (d) Chinn, M. S.; Heinekey, D. M. *J. Am. Chem. Soc.* **1990**, *112*, 5166–5175. (e) Bullock, R. M.; Song, J.-S.; Szalda, D. J. *Organometallics* **1996**, *15*, 2504–2516. (f) Ontko, A. C.; Houllis, J. F.; Schnabel, R. C.; Roddick, D. M.; Fong, T. P.; Lough, A. J.; Morris, R. H. *Organometallics* **1998**, *17*, 5467–5476. (g) Papish, E. T.; Magee, M. P.; Norton, J. R. In *Recent Advances in Hydride Chemistry*; Peruzzini, M., Poli, R., Eds.; Elsevier: New York, 2001; pp 39–74.

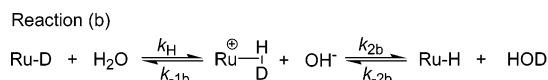
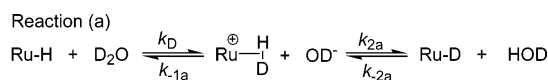
(47) (a) Gaus, P. L.; Kao, S. C.; Darensbourg, M. Y.; Arndt, L. W. *J. Am. Chem. Soc.* **1984**, *106*, 4752–4755. (b) Feracin, S.; Bürgi, T.; Bakhumtov, V.; Eremenko, I.; Vorontsov, E. V.; Vimenitis, A. B.; Berke, H. *Organometallics* **1994**, *13*, 4194–4202.

(48) Normally, these reactions are viewed as proton transfers; however, Scheme 2 could also be viewed as a σ bond metathesis.



range of the initial product of protonation, CpRu(PTA)₂(H₂)⁺.⁴⁹ As we can observe a potential intermediate for the reaction in Scheme 1, we favor proton transfer as the mechanism of H/D exchange.

From the data we have collected it is possible to extract the rate constants for the protonation of **2** by D₂O and the protonation of **2D** by H₂O, thus enabling calculation of a primary kinetic isotope effect (KIE) for the H/D exchange reaction. The rate constants k_H and k_D may be determined by taking k_{obs} from reactions (a) and (b) and applying a fractional probability factor (F) to account for the percentage of time that formation of the Ru(HD)⁺ intermediate leads to observable isotopic exchange, neglecting secondary isotope effects. We have used a value of F reported by Norton et al. for the protonation of CpW(CO)₂(PMe₃)H with 4-*tert*-butyl-*N,N*-dimethylanilinium; $F_a \approx 0.625$ for reaction a and $F_b \approx 0.375$ for reaction b; see eqs 1 and 2.^{50,51} Dividing k_{obs} by F gives rate constants for k_H and k_D at 308 K of 3.30×10^{-3} and $4.16 \times 10^{-4} \text{ s}^{-1}$, respectively, and a normal KIE (k_H/k_D) of ~ 7.9 . The KIE calculated compares reasonably well to the expected isotope effect, 10.5 at 308 K, for H⁺ (D⁺) transfer from H₂O (D₂O), ignoring secondary isotope effects and assuming a linear transition state for the transfer.^{51–53}



$$F_a = \frac{k_{2a}}{k_{-1a} + k_{2a}} \approx 0.625 \quad (1)$$

$$F_b = \frac{k_{2b}}{k_{-1b} + k_{2b}} = \frac{k_{-1a}}{k_{-1a} + k_{2a}} = 1 - F_a \approx 0.375 \quad (2)$$

Kuo et al. observed H/D exchange of Cp₂Mo(H)(OTf) with D₂O and reported a k_{obs} of $1.14 \times 10^{-4} \text{ s}^{-1}$ at 45°,

(49) Frost, B. J.; Mebi, C. A. Manuscript in preparation.

(50) Note that since we are ignoring secondary isotope effects, $k_{2a} = k_{-1b}$ and $k_{2b} = k_{-1a}$.

approximately 4.5 times smaller than k_{obs} for H/D exchange in **2**.⁵⁴ Also noted in this study was that the rate of H/D exchange was “relatively temperature independent” and that the rate was faster at low pH.⁵⁴ Atwood and co-workers have also reported H/D exchange between a metal hydride and D₂O: Ir(CO)(Cl)(H)₂(TPPTS)₂ undergoes slow H/D exchange with D₂O. Of note is that the two hydrides, H_a *trans* to Cl and H_b *trans* to CO, exchange at different rates ($t_{1/2}(\text{H}_a) = 20 \text{ h}$; $t_{1/2}(\text{H}_b) = 40 \text{ h}$), with the more shielded hydride exchanging faster.⁵⁵

Conclusions

We have reported here the isolation and characterization of a water-soluble half-sandwich Ru(II) hydride. The crystal structure of CpRu(PTA)₂H is described and is to the best of our knowledge the first structurally characterized water-soluble CpRu(PR₃)₂H complex reported in the literature. This compound has been reported to be involved in the hydrogenation of α,β -unsaturated ketones.³¹ CpRu(PTA)₂H when dissolved in D₂O undergoes a rapid H/D exchange reaction, yielding CpRu(PTA)₂D. Activation parameters for this reaction were found to be $\Delta H^\ddagger = 68 \pm 2 \text{ kJ/mol}$ and $\Delta S^\ddagger = -94 \pm 7 \text{ J/mol}\cdot\text{K}$. Coupled with a normal kinetic isotope effect, $k_H/k_D = 7.9$, we propose a mechanism involving protonation of **2** by water, generating a dihydrogen intermediate, followed by deprotonation of the intermediate by the resultant hydroxide ion. Currently we are exploring the ability of the CpRu(PTA)₂H complex described herein to catalyze the hydrogenation of C=O, C=C, and C=N bonds and are exploring the nature of the protonated intermediate, CpRu(PTA)₂(H)₂⁺, mentioned herein.

Acknowledgment. This research was supported by the University of Nevada (JFRA). We thank Cytec for the generous gift of P(CH₂OH)₄Cl. Financial support from the National Science Foundation (CHE-0226402) is acknowledged for funding for the X-ray diffractometer. The authors would also like to thank J. R. Norton for helpful discussions regarding isotope effects.

Supporting Information Available: Complete details of the crystallographic study (PDF and CIF) and NMR spectra of the reaction of **2D** with H₂O. This material is available free of charge via the Internet at <http://pubs.acs.org>.

OM049501+

(51) Papish, E. T.; Rix, F. C.; Spetseris, N.; Norton, J. R.; Williams, R. D. *J. Am. Chem. Soc.* **2000**, *122*, 12235–12242.

(52) Cheng, T.-Y.; Bullock, R. M. *J. Am. Chem. Soc.* **1999**, *121*, 3150–3155.

(53) Edidin, R. T.; Sullivan, J. M.; Norton, J. R. *J. Am. Chem. Soc.* **1987**, *109*, 3945–3953.

(54) Kuo, L. Y.; Weakley, T. J. R.; Awana, K.; Hsia, C. *Organometallics* **2001**, *20*, 4969–4972.

(55) Paterniti, D. P.; Roman, P. J., Jr.; Atwood, J. D. *Organometallics* **1997**, *16*, 3371–3376.